Article

Cell Metabolism

Reduced Insulin Production Relieves Endoplasmic Reticulum Stress and Induces β Cell Proliferation

Graphical Abstract

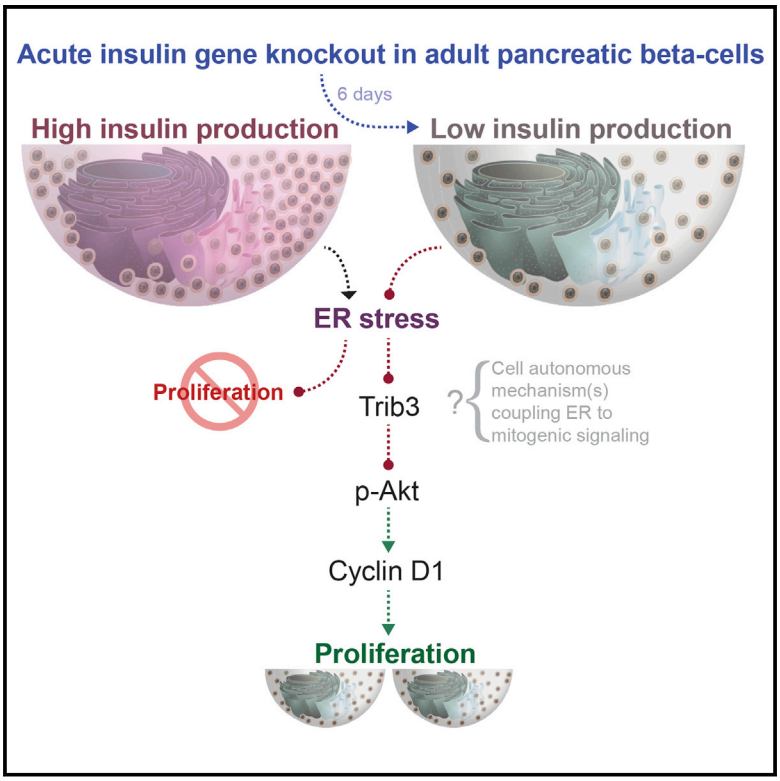

Authors

Marta Szabat, Melissa M. Page, Evgeniy Panzhinskiy, ..., Corey Nislow, Timothy J. Kieffer, James D. Johnson

Correspondence

James.D.Johnson@ubc.ca

In Brief

Szabat et al. show that the normally high rate of insulin production acts as a brake on adult β cell proliferation in mice. Reducing this burden via acute deletion of the insulin gene relieves baseline ER stress, increases mitogenic signaling, and promotes cell-cycle progression in a cell-autonomous manner.

Highlights

- Acute reduction of insulin production reverses baseline ER stress
- Loss of insulin production reduces Trib3 and hyper-activates Akt
- Reduced insulin production increases β cell proliferation cell autonomously
- Insulin knockout induces glucagon mis-expression via hyperglycemia

Szabat et al., 2016, Cell Metabolism *23*, 179–193
January 12, 2016
http://dx.doi.org/10.1016/j.cmet.2015.10.016

Cell Metabolism
Article

Reduced Insulin Production Relieves Endoplasmic Reticulum Stress and Induces β Cell Proliferation

Marta Szabat,[1] Melissa M. Page,[1] Evgeniy Panzhinskiy,[1] Søs Skovsø,[1] Majid Mojibian,[1] Juan Fernandez-Tajes,[2] Jennifer E. Bruin,[1] Michael J. Bround,[1] Jason T.C. Lee,[1] Eric E. Xu,[3] Farnaz Taghizadeh,[1] Shannon O'Dwyer,[1] Martijn van de Bunt,[2] Kyung-Mee Moon,[4] Sunita Sinha,[5] Jun Han,[6] Yong Fan,[7] Francis C. Lynn,[3] Massimo Trucco,[7] Christoph H. Borchers,[6] Leonard J. Foster,[4] Corey Nislow,[5] Timothy J. Kieffer,[1] and James D. Johnson[1,*]
[1]Department of Cellular and Physiological Sciences, Diabetes Research Group, Life Sciences Institute, University of British Columbia, BC V6T1Z3, Canada
[2]Wellcome Trust Centre for Human Genetics, University of Oxford, Oxford OX3 7BN, UK
[3]Child and Family Research Institute, University of British Columbia, BC V5Z 4H4, Canada
[4]Centre for High-Throughput Biology
[5]Faculty of Pharmaceutical Sciences
University of British Columbia, BC V6T 1Z3, Canada
[6]UVic-Genome BC Proteomics Centre, University of Victoria, BC V8Z 7X8, Canada
[7]Institute of Cellular Therapeutics, Allegheny Health Network, Pittsburgh, PA 15212-4772, USA
*Correspondence: James.D.Johnson@ubc.ca
http://dx.doi.org/10.1016/j.cmet.2015.10.016

SUMMARY

Pancreatic β cells are mostly post-mitotic, but it is unclear what locks them in this state. Perturbations including uncontrolled hyperglycemia can drive β cells into more pliable states with reduced cellular insulin levels, increased β cell proliferation, and hormone mis-expression, but it is unknown whether reduced insulin production itself plays a role. Here, we define the effects of ~50% reduced insulin production in *Ins1*$^{-/-}$:*Ins2*$^{f/f}$:*Pdx1*Cre^{ERT}:mTmG mice prior to robust hyperglycemia. Transcriptome, proteome, and network analysis revealed alleviation of chronic endoplasmic reticulum (ER) stress, indicated by reduced *Ddit3*, *Trib3*, and *Atf4* expression; reduced *Xbp1* splicing; and reduced phospho-eIF2α. This state was associated with hyper-phosphorylation of Akt, which is negatively regulated by Trib3, and with cyclinD1 upregulation. Remarkably, β cell proliferation was increased 2-fold after reduced insulin production independently of hyperglycemia. Eventually, recombined cells mis-expressed glucagon in the hyperglycemic state. We conclude that the normally high rate of insulin production suppresses β cell proliferation in a cell-autonomous manner.

INTRODUCTION

Pancreatic β cells are long-lived specialized secretory cells tasked with the production of all circulating insulin, which is essential for healthy long-term survival (Mezza and Kulkarni, 2014). When stressed, β cells can exit their mature differentiated state into states of dysfunction and dedifferentiation, including conditions wherein β cells have little to no insulin protein (Szabat et al., 2012; Weir et al., 2013). Dedifferentiation has been proposed as an important mechanism of β cell dysfunction in diabetes (Akirav et al., 2008; Brereton et al., 2014; Guo et al., 2013; Talchai et al., 2012; Wang et al., 2014; Weir et al., 2013) but remains poorly understood. For example, it is not clear whether the loss of insulin production in adult β cells is causally linked to proliferation, dedifferentiation, or transdifferentiation (Szabat et al., 2012). The inverse relationship between differentiation and proliferation is illustrated by the demonstration that halting proliferation in a human β cell line dramatically increased insulin content (Scharfmann et al., 2014), but it is not known whether inhibiting insulin production alone might be sufficient to increase adult β cell proliferation. Germ-line disruption of both insulin genes in mice caused severe diabetes and neonatal death, precluding analysis of adult β cells in that model (Duvillié et al., 2002). In post-natal mice, near complete β cell ablation increases β cell proliferation (Nir et al., 2007) and plasticity of other islet cell types (Chera et al., 2014; Thorel et al., 2010), but it is not clear to what extent the effects in these acute injury models are due to the loss of insulin, rather than the loss of β cells. To address the question of whether the burden of producing large quantities of insulin normally suppresses proliferation in a cell-autonomous manner, one must acutely reduce insulin in adult β cells. Such an animal model would provide, for the first time, an opportunity to study the fates of cells that had lost their ability to produce their primary secreted protein.

In the present study, we use transcriptomics, proteomics, and metabolomics to define systems-wide changes that accompany the acute loss of insulin production in adult mouse β cells following deletion of two floxed *Ins2* alleles in mice already lacking both *Ins1* alleles. This unbiased survey identified a reversal of baseline ER stress in cells with reduced insulin production. We observed a significant increase in proliferation prior to the inevitable robust hyperglycemia in this model and

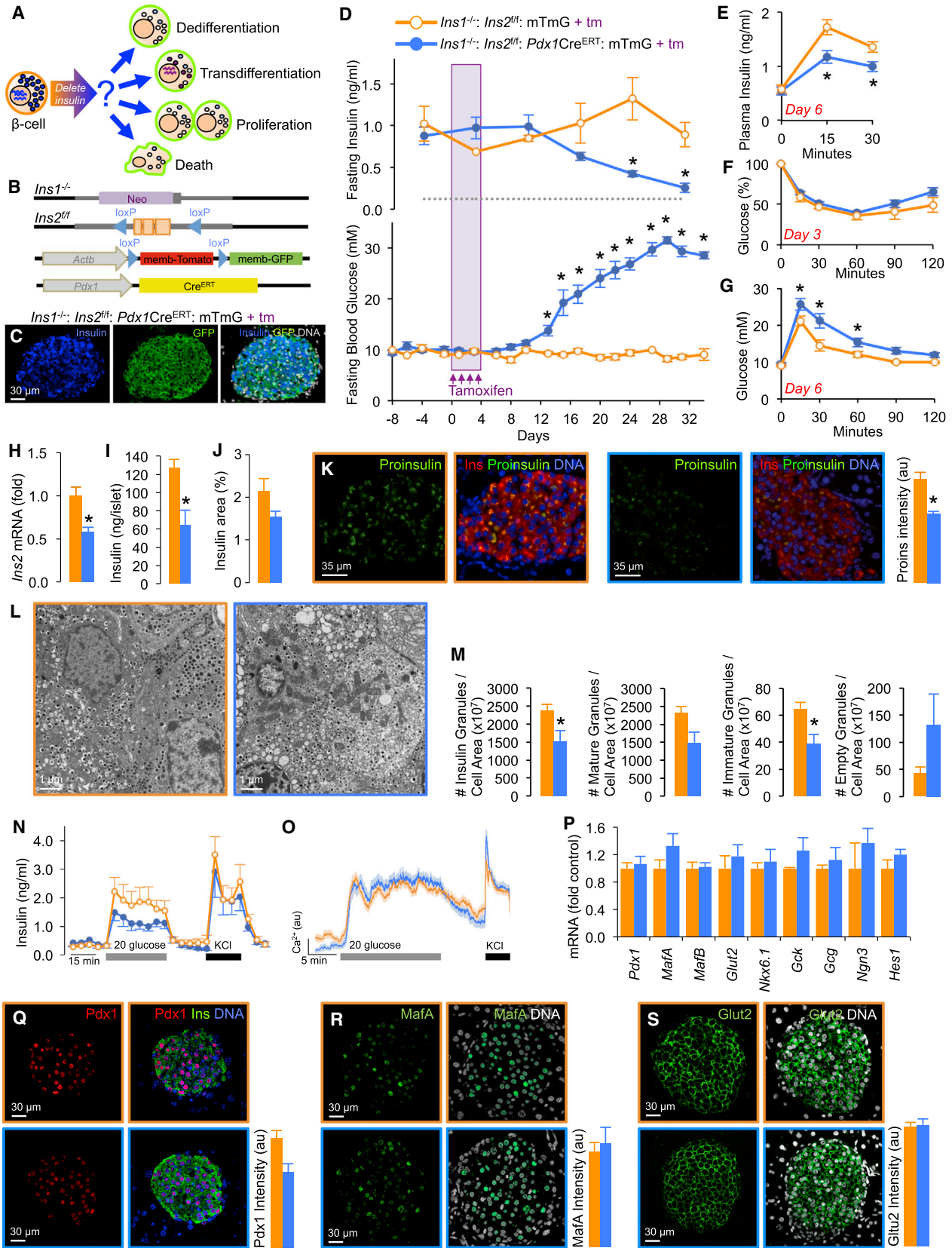

(legend on next page)

used complementary experiments with controlled glucose to demonstrate the cell-autonomous nature of this effect. We also observed an increased number of insulin gene knockout β cells that mis-expressed glucagon protein, but only after robust hyperglycemia. Our results provide the first evidence that normal insulin production directly constrains β cell proliferation.

RESULTS AND DISCUSSION

Physiological Characterization of Mice with Acute Islet Insulin Gene Knockout

The effects of reducing insulin production in adult β cells are unknown (Figure 1A). To distinguish between possible β cell fates, we generated a mouse model with conditional deletion of *Ins2* (Fan et al., 2009) on an *Ins1*-null background (Duvillié et al., 2002), where β cell selective tamoxifen-inducible Cre is driven by a *Pdx1* promoter fragment (*Pdx1*Cre^{ERT}) (Figure 1B). This Cre "deleter" allele resulted in virtually complete recombination, as measured by the antibody staining against membrane targeted GFP from the mTmG reporter allele (Muzumdar et al., 2007) (~99%; Figure 1C). Acute *Ins2* gene knockout resulted in the expected loss of circulating insulin and sustained diabetes in all experimental *Ins1*$^{-/-}$:*Ins2*$^{f/f}$:*Pdx1*Cre^{ERT}:mTmG but not in control *Ins1*$^{-/-}$:*Ins2*$^{f/f}$:mTmG mice (Figure 1D). Remarkably, the onset of hyperglycemia and insulinopenia was delayed by 14 ± 4 days after the initiation of *Ins2* deletion by tamoxifen. This delay is consistent with the abundance and stability of *Ins2* mRNA, the large amount of stored insulin, and the functional excess of β cell mass (Tillmar et al., 2002). While islets can express hundreds of growth factors, cytokines, and hormones (Yang et al., 2011b, 2015), our data confirm that insulin is non-redundant for glucose homeostasis in adult mice.

Six days after tamoxifen initiation, a time when fasting insulin and glucose were normal (Figure 1D), in vivo glucose-stimulated insulin secretion was reduced by ~50%, insulin sensitivity was normal, and glucose tolerance was only mildly impaired (Figures 1E–1G). We addressed the state of β cells with reduced insulin production at the 6-day time point to focus on potential cell-autonomous effects independent of altered circulating insulin and sustained, robust hyperglycemia (Figure 1D), which have profound effects on β cell differentiation state (Brereton et al., 2014; Wang et al., 2014). Six days after *Ins2* allele recombination, islets had roughly half their reserves of *Ins2* mRNA and insulin protein content (Figures 1H and 1I). The relative area of insulin immunoreactivity, a composite of insulin content and β cell mass, was not significantly different at this time point (Figure 1J). Although stored insulin was readily apparent by immunofluorescence, pro-insulin was significantly decreased (Figure 1K), consistent with a robust reduction in new insulin synthesis. Perhaps expectedly, electron microscopy illustrated that β cells with reduced insulin production had fewer mature dense core granules and fewer immature/new insulin granules, while the overall ultrastructural morphology was normal (Figures 1L and 1M). Dynamic analysis of insulin secretion demonstrated that glucose-stimulated insulin secretion was reduced by ~50%, while basal and KCl-stimulated insulin secretion were unchanged (Figure 1N). The observations that fasting/basal insulin were unchanged in vivo and in vitro, but glucose-stimulated insulin secretion was reduced, are consistent with the concept that newer insulin is selectively released by glucose and older stored insulin supports basal glucose homeostasis. Halban previously reported that newly synthesized insulin was preferentially released, but they did not find a further preferential release with increased glucose (Halban, 1982). Recently, in vitro studies have suggested that the most recently synthesized insulin is selectively released upon glucose stimulation (Ivanova et al., 2013), and our data provide in vivo support for this concept, although additional studies are clearly warranted on this topic. Notably, β cells with reduced insulin production were otherwise fully functional, with identical Ca^{2+} responses to 20 mM glucose and 30 mM KCl (Figure 1O). Reduction of insulin production also did not appear to lead to β cell dedifferentiation, based on mRNA and protein levels of known differentiation/maturity genes (Szabat et al., 2010) (Figures 1P–1S). Collectively, our data demonstrate that 6 days after the acute abrogation of insulin production, pancreatic β cells remain grossly normal while retaining some stored insulin that enables normal fasting glucose homeostasis.

Figure 1. Adult Insulin Gene Knockout β Cells Produce and Release Less Insulin but Are Otherwise Normally Differentiated

(A) Schematic of possible fates of insulin gene knockout β cells.

(B) Alleles required for conditional *Ins2* deletion on an *Ins1*-null background and lineage-tracing with membrane-targeted eGFP marks cells after tamoxifen-inducible *Pdx1*-driven Cre-mediated recombination of membrane-targeted tdTomato.

(C) Near complete Cre-recombination efficiency (~99% of β cells are GFP-positive) and residual insulin stores in *Ins1*$^{-/-}$:*Ins2*$^{f/f}$:*Pdx1*Cre^{ERT}:mTmG islets 6 days after tamoxifen. Unless otherwise stated, *Ins1*$^{-/-}$:*Ins2*$^{f/f}$:*Pdx1*Cre^{ERT}:mTmG treatment mice with insulin gene knockout were compared with littermate *Ins1*$^{-/-}$:*Ins2*$^{f/f}$:mTmG control mice throughout this study, with both groups injected with tamoxifen.

(D) Plasma insulin (n = 3, 14; control replicates listed 1st throughout) and blood glucose (n = 6, 14) were measured after a 4 hr fast. Gray line indicates the limit of detection. No changes in body weight between control and experimental groups were observed (not shown).

(E–G) Glucose-stimulated insulin secretion (n = 3, 5), insulin tolerance (n = 4, 7), glucose tolerance (n = 6, 12) tests at the indicated time points.

(H) *Ins2* mRNA quantification by qPCR at the 6-day time point (as are all subsequent data unless otherwise specified) (n = 8, 9).

(I) Insulin content in isolated islets (n = 3).

(J) Pancreatic insulin-positive area (n = 3).

(K) Proinsulin immunofluorescence (n = 3).

(L and M) Electron microscopy and quantification of granule populations. Two representative images from three samples of each group.

(N) Dynamic analysis of insulin secretion by perifusion (n = 6).

(O) Average Ca^{2+} responses to 20 mM glucose and 30 mM KCl (n > 100 cells in each group).

(P) qPCR analysis of islet cell differentiation markers (n = 8, 9).

(Q–S) Imaging and quantification of Pdx1, MafA, and Glut2 Immunofluorescence (n = 3). *$p < 0.05$. Orange and blue borders around immunofluorescence images represent *Ins1*$^{-/-}$:*Ins2*$^{f/f}$:mTmG controls and *Ins1*$^{-/-}$:*Ins2*$^{f/f}$:*Pdx1*Cre^{ERT}:mTmG experimental samples, respectively. All error bars represent SEM of pooled data.

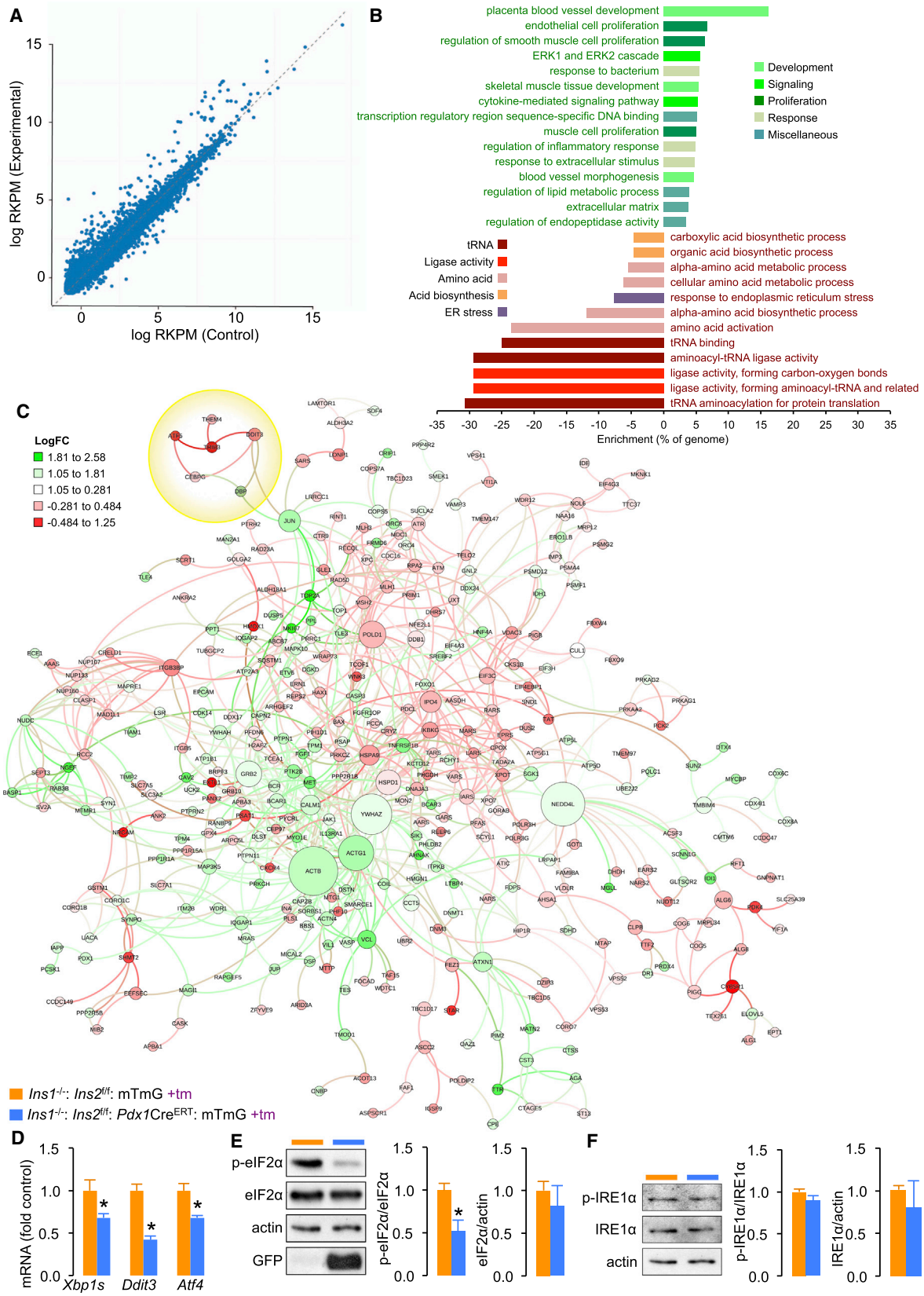

(legend on next page)

Transcriptomic and Network Analysis of Islets with Reduced Insulin Production

To assess the effect of acute insulin gene knockout on the whole transcriptome, we conducted RNA-sequencing, gene enrichment, and network analysis on islets isolated 6 days after tamoxifen initiation (Figure 2A; Table S1). We identified 800 differentially expressed genes with a q value of < 0.001. Among the 150 most increased mRNAs (>2-fold increased), there was a significant enrichment for genes with functions related generally to development, proliferation, and transduction of extracellular signals in other tissues (Figure 2B). For example, insulin gene knockout islets exhibited enrichment for mRNAs associated with development, cellular plasticity, and/or survival, including *Notch3* (Dror et al., 2007; Mezza and Kulkarni, 2014), *Foxo1* (Talchai et al., 2012), and *Npas4* (Sabatini et al., 2013), as well as genes that promote proliferation, such as *Cdk1*, *Cdk14*, and *Cdkl5*. Among the 150 most decreased mRNAs (>2-fold decreased), there was a significant enrichment for tRNA genes, genes involved in amino acid homeostasis, and the ER stress response. In particular, we noted a coordinated decrease in an ER stress response sub-network involving *Ddit3*, *Atf4*, *Atf5*, *Fam129a*, and *Trib3*, which is an Akt inhibitor downstream of the Atf4/Ddit3 pathway (Du et al., 2003; Ohoka et al., 2005) (Figure 2B, yellow circle in Figure 2C; Table S1).

We used protein-protein interaction network modeling to translate global changes in significant differential mRNA expression (q < 0.001) into predictions of important functional networks (Figure 2C). A highly downregulated sub-network containing Trib3, Ddit3, Atf5, Cebpg, and Them4 was connected to the main network through the upregulated *Dbp* gene and the highly connected node, Jun (yellow circle in Figure 2C). The DNA polymerase, Pold1, decreased in insulin gene knockout islets, was connected to Foxo1 and Eif4a3 and also to Hspd1 and Grb2, two other highly connected nodes. Many genes were connected through Actb and Actg1, suggesting alterations in networks modulated by the actin cytoskeleton in insulin gene knockout cells. Other highly connected nodes in the network were Nedd4L, a E3 ubiquitin ligase, and Ywhaz, a signaling scaffold we have previously implicated in β cell survival (Lim et al., 2013) and adipocyte progenitor proliferation (Lim et al., 2015). Together, the network modeling pointed to key changes in core biosynthetic pathways, the transduction of extracellular signals, and stress signaling.

We further investigated the downregulation of ER stress in this model and found significant reductions in spliced *Xpb1* mRNA and phosphorylated eIF2α (Figures 2D and 2E). We did not observe consistent differences in IRE1α phosphorylation (Figure 2F). Our observations are consistent with the concept that insulin production is normally a source of chronic, sub-threshold ER stress (Back and Kaufman, 2012; Vander Mierde et al., 2007) that was alleviated by knocking out a gene whose transcription accounts for more mRNA than the next 500 most highly expressed transcripts combined (Table S1).

Proteomic and Network Analysis of Islets with Reduced Insulin Production

We next assessed the effects of reduced insulin production using semiquantitative proteomic analysis, which allowed us to assess 2,101 proteins with high confidence (Figure 3; Table S2). Unlike the RNAseq analysis, it is not currently possible to quantify every protein in these cells. Nevertheless, analysis of this partial proteome complemented the transcriptome analysis, with significant changes in key cellular proteostasis components (Figures 3A and 3B). The 150 most increased proteins were significantly enriched for components of the proteosome, including Psma4, which was increased ~4-fold (Figure 3A). The 150 most decreased proteins were significantly enriched for ribosome components, proteins involved in the ER and Golgi. The list of decreased proteins showed a significant enrichment for proteins involved in translation, although one factor, Eif4e, was increased ~3-fold (Figure 3A). Overall, the top three significantly altered Reactome pathways from the proteomics data were related to translation (Table S3). Collectively, our proteome data demonstrate that insulin gene deletion results in profound changes to networks involved in protein synthesis, processing, trafficking, and degradation. This suggests the possibility that specific translational components are linked to insulin production, a concept that will require further study.

We also generated a protein-protein interaction network from the top 150 increased and 150 decreased proteins, but in this case, we also included the first-degree interactors of these proteins. This means that the resulting network contains proteins not found to be differentially abundant in the proteomic analysis but might otherwise interact and mediate signaling events. Indeed, the significantly changed pathways in this network provided unexpected insights into protein networks altered after insulin gene knockout (Figures 3C and 3D; Table S4). Hdac2, increased ~6-fold in insulin gene knockout islets, was the most connected node, with 60 interacting proteins including key islet transcription factors Pdx1, Tcf7l2, Atf3, and Yy1. Yy1 has recently been implicated in insulinoma (Cromer et al., 2015). Another highly connected sub-network involved the Set nuclear oncogene, which was significantly increased, and its binding partner the Nme1 tumor suppressor, which was decreased (Switzer et al., 2011). A sub-network of small G-proteins (Rab8a, Rab3d, and Rab6a) involved in intra-organelle transport was also significantly decreased. Nedd8, a small ubiquitin-like protein, was reduced and connected to Cul1, Cul5, Senp8,

Figure 2. Transcriptome and Network Analysis of Islets with Reduced Insulin Production

(A) RNAseq data from islets isolated from *Ins1*$^{-/-}$:*Ins2*$^{f/f}$:*Pdx1*Cre^{ERT}:mTmG mice and littermate control *Ins1*$^{-/-}$:*Ins2*$^{f/f}$:mTmG mice, 6 days after tamoxifen initiation. See Table S1 for a sortable list of significantly changed mRNAs (fold change > |2|, significance cutoff q < 0.001; n = 9, 7).

(B) Illustration of the major upregulated gene categories (green words) and downregulated gene categories (red words). Significantly enriched (FDR < 0.05) Panther Gene Ontology Functions are expressed of the fraction represented Functions over the total number of genes in the genome in that Function category.

(C) Analysis of a protein-protein interaction network assembled from RNAseq data. Node size represents "betweeness" and node color reflects whether its mRNA is increased (green) or decreased (red). Intermediate colors reflect moderate fold changes. *p < 0.05.

(D) qPCR analysis of spliced *Xpb1*, *Ddit3*, and *Atf4* mRNA from independent samples (n = 6–9).

(E and F) Immunoblots and quantification of the phosphorylation and abundance of eIF2α and IRE1α (n = 16, 10). All error bars represent SEM of pooled data.

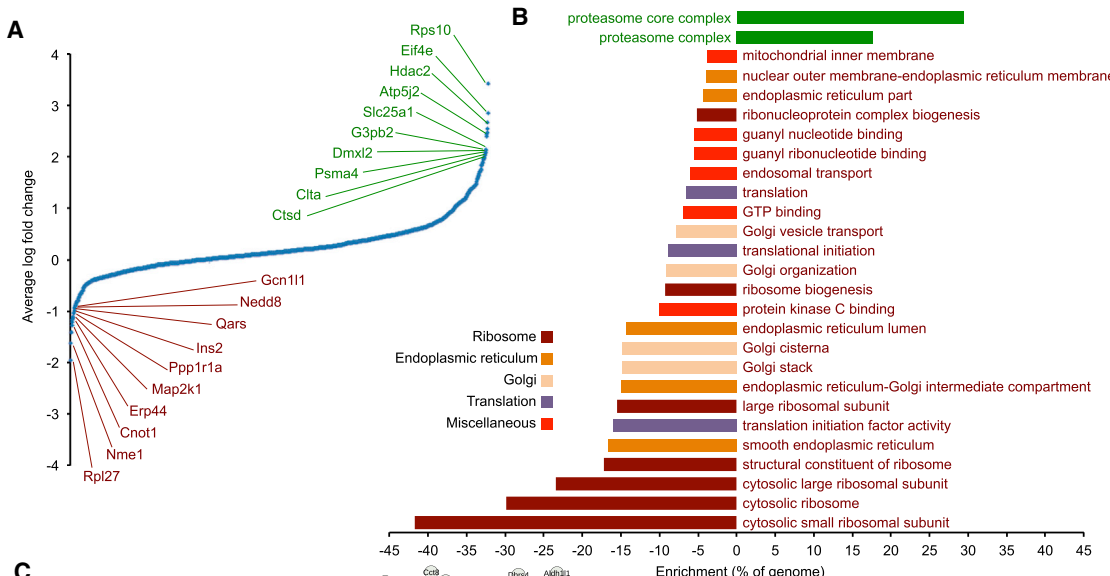

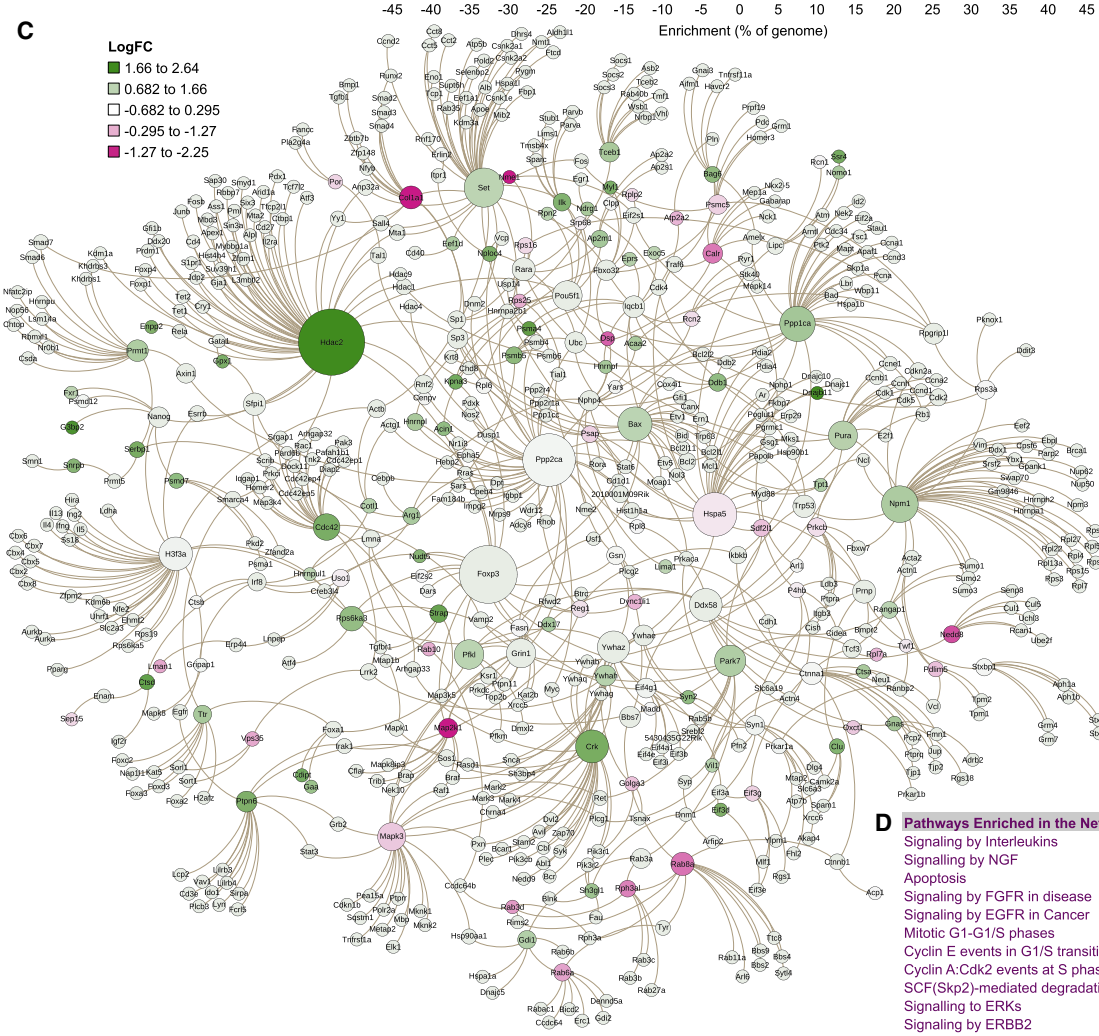

D

Pathways Enriched in the Network	P value
Signaling by Interleukins	1E-13
Signalling by NGF	1E-12
Apoptosis	9E-11
Signaling by FGFR in disease	4E-08
Signaling by EGFR in Cancer	5E-08
Mitotic G1-G1/S phases	6E-08
Cyclin E events in G1/S transition	1E-07
Cyclin A:Cdk2 events at S phase entry	1E-07
SCF(Skp2)-mediated degradation of p27/p21	1E-06
Signalling to ERKs	1E-06
Signaling by ERBB2	2E-06
Signaling by PDGF	2E-06
Axon guidance	3E-06
p53-Dependent G1 DNA Damage Response	5E-06

(legend on next page)

and Uchl3 (Chu et al., 2012). Nedd8 has been reported to be involved in cell cycle, apoptosis, ribosomal stress, and receptor tyrosine kinase signaling (Enchev et al., 2015). Hdac2 abundance can be controlled by neddylation (Pandey et al., 2015).

Similar to the network derived from mRNA expression, this network revealed alterations in signal transduction pathways. In particular, MAP kinase signaling components were identified as important network hubs. Ywhaz, a regulator of both MAP kinase and Akt signaling, was highly connected in both networks. Crk (~3-fold increased), an upstream activator of Akt (Akagi et al., 2000), connected Ywhaz as well as multiple kinases to the network. Map2k1 (Mek1) and Mapk3 (Erk1), which were both decreased, were also highly connected nodes. Our network analysis also pointed to an important role for phosphatases. Ppp1ca, the catalytic subunit of PP1, plays a prominent role in cell division (Wurzenberger and Gerlich, 2011) and was connected in our network with Rb, PCNA, and multiple cyclins. Thus, global analysis of our protein-protein interaction networks revealed connections to multiple cell-cycle-related signaling pathways and pointed toward a positive effect on cell proliferation in insulin gene knockout islets.

Metabolomic Analysis of Islets with Reduced Insulin Production

Transcriptomic, proteomic, and network analysis of islets with reduced insulin production revealed marked global downregulation of protein synthesis machinery, as well as other networks expected to consume cellular energy. We therefore employed targeted metabolomic analysis to assess the effects of insulin gene knockout on cellular metabolic pathways. Islets with reduced insulin production exhibited increased levels of the energy storing nucleotides (Figure 4A). Increased high-energy phosphates (ATP and ADP) were not associated with upregulation in glycolytic or Kreb's cycle intermediates (Figure 4B). Interestingly, metabolomic profiling revealed significant decreases in the pentose-phosphate shunt intermediate, ribose 5-phosphate, and acetyl-CoA (Figure 4B). Collectively, these data demonstrate that β cells with reduced insulin production accumulate high-energy phosphates, possibly via energy sparing mechanisms rather than increased metabolism. However, more detailed metabolomic analyses and flux measurements are required to make strong conclusions regarding the metabolic state of these islets.

Despite the fact that insulin is the major protein product of β cells, the total amount of protein observed in islet lysates was not reduced in insulin gene knockout islets (Figure 4C). This suggested that the translation of the other β cell proteins may have been upregulated, perhaps de-repressed. We therefore evaluated the protein synthesis rate of the remaining mRNAs using S^{35} labeling and found that it was modestly increased (Figure 4D). This was associated with a broad decrease in cellular amino acids levels (Figure 4E). These observations are consistent with a model by which ATP sparing enables the increased rate of global protein synthesis of the remaining non-insulin proteins (Figure 4F).

Activation of Mitogenic Signaling in β Cells with Reduced Insulin Production

The network analysis from both the transcriptomic and proteomic datasets pointed to significant alterations in β cell signal transduction pathways. Islets with reduced insulin production had a ~2-fold reduction in Map2k1 (Mek1) protein (Figure 3A), as well as modest decreases in Mapk1 (Erk2) and Mapk3 (Erk1). Moreover, the sub-cellular distribution of Erk1/2 was dramatically altered in insulin gene knockout islets, with a relative loss of nuclear localization, possibly indicative of pathway inactivation (Figure 5A). We also examined the protein localization of Trib3, which was identified in the RNA-sequencing studies and associated network analysis as a key component of the reduced ER stress network (Figure 2). Trib3 immunoreactivity, which was normally strong and clearly nuclear in the control islets, exhibited weaker, less organized localization in the insulin gene knockout islets (Figure 5B). Trib3 is an established negative regulator of Akt (Du et al., 2003), and we observed altered sub-cellular Akt localization and hyper-phosphorylation of Akt at serine 473 in insulin gene knockout islets (Figures 5C and 5D). In addition to Trib3, our proteomic and network analysis suggest that multiple upstream inputs, including Hdac2 (Noh et al., 2014), Crk (Akagi et al., 2000), and Set/Nme1 (Switzer et al., 2011) could combine to increase Akt phosphorylation (Figure 5E). Our results are consistent with the known negative effects of ER stress on Akt signaling in β cells (Wrede et al., 2002). Previous studies have established that Akt hyperactivity is sufficient to increase β cell proliferation via cyclinD1 (Bernal-Mizrachi et al., 2001; Fatrai et al., 2006), so we assessed the number of β cells with high levels of this critical cell-cycle protein. Indeed, insulin gene knockout islets had a >2-fold increase in cyclinD1-positive β cells, when compared with controls (Figure 5F). CyclinD1 is known to play a key role in post-natal β cell proliferation (Kushner et al., 2005). Together, these data point to the activation of signaling pathways that favor proliferation in β cells.

Cell-Autonomous Increase in Proliferation in β Cells with Reduced Insulin Production

Our data at 6 days after insulin gene knockout clearly showed that a specific reduction in insulin synthesis induced profound changes to the transcriptome and proteome, including the

Figure 3. Proteome and Network Analysis of Islets with Reduced Insulin Production

(A) Proteomic analysis of islets isolated from *Ins1*$^{-/-}$:*Ins2*$^{f/f}$:*Pdx1*Cre^{ERT}:mTmG mice and littermate control *Ins1*$^{-/-}$:*Ins2*$^{f/f}$:mTmG mice, 6 days after tamoxifen initiation. Normalized data are log2 fold-change (n = 3). See Table S2 for a sortable list of raw proteomic data. GFP, the most increased protein, is not shown.

(B) Illustration of the major upregulated protein categories (green words) and downregulated protein categories (red words). Significantly enriched (FDR < 0.05) Panther Gene Ontology Functions are expressed of the fraction represented over the total number of Function genes in the genome.

(C) Protein-protein interaction network assembled from 150 most increased and 150 most decreased proteins, as well as their first-order interacting proteins. Node size represents "betweeness" and node color reflects whether the protein is increased (green) or decreased (magenta). Intermediate colors reflect moderate fold changes.

(D) Selected enriched pathways in the protein-protein interaction network highlights changes in signal transduction and cell-cycle control. A complete list of significantly enriched pathways can be found in the Table S4.

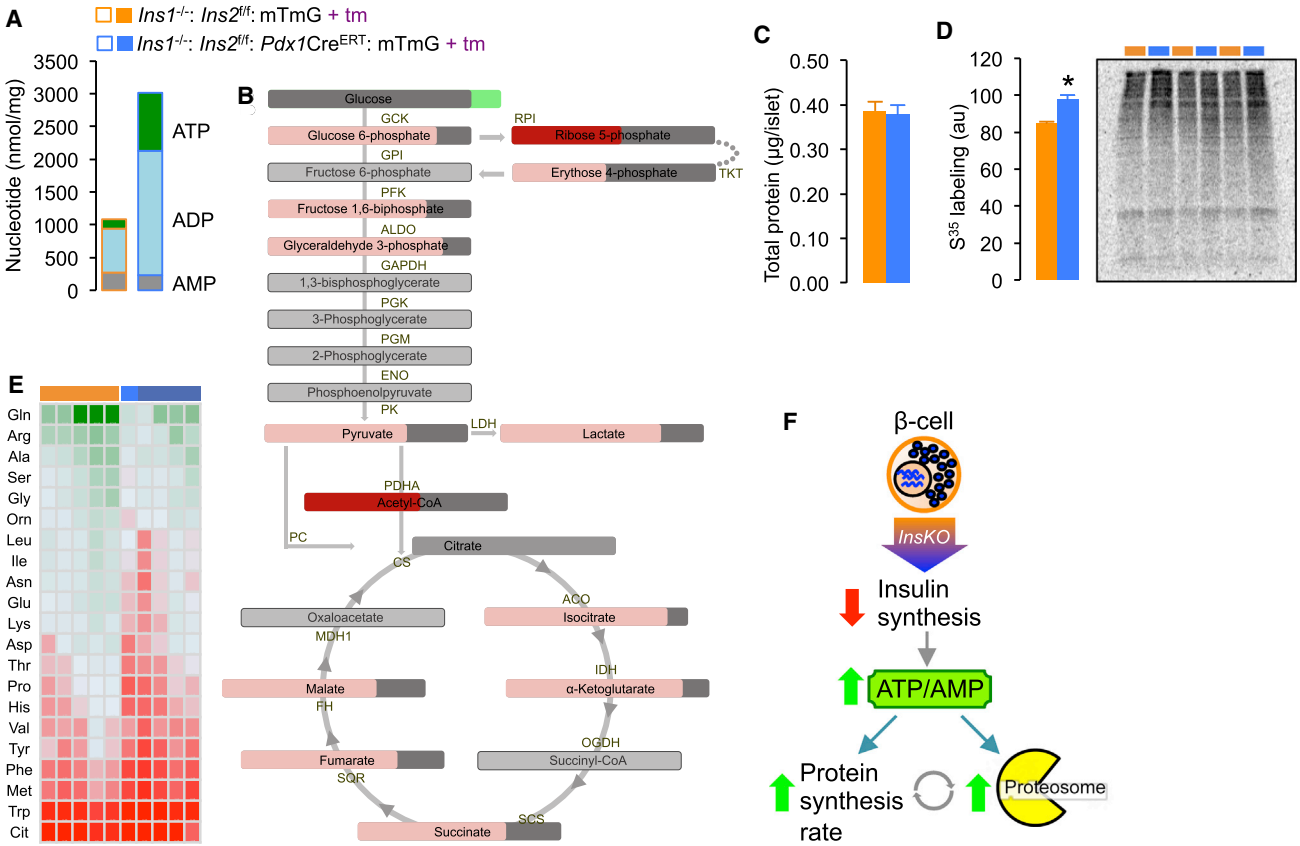

Figure 4. Metabolomic Analysis of Islets with Reduced Insulin Production

(A) Effects of halted insulin production on AMP, ADP, and ATP levels in islets isolated from *Ins1*$^{-/-}$:*Ins2*$^{f/f}$:*Pdx1*Cre^{ERT}:mTmG mice and littermate control *Ins1*$^{-/-}$:*Ins2*$^{f/f}$:mTmG mice, 6 days after tamoxifen initiation.

(B) Effects of insulin production loss on metabolic intermediates of glycolysis, the Kreb's cycle, and the pentose-phosphate shunt. Red or green bars reflect percentage change, relative to gray bars, of significantly altered metabolites. Light red denotes metabolites that were measured but not statistically different (n = 5).

(C) Total protein levels in isolated islets (n = 12).

(D) Protein synthesis rate measured by S^{35} labeling (n = 8).

(E) Effects of insulin production loss on steady-state levels of amino acids.

(F) Working model of altered proteostasis in islets with reduced insulin production, taking into account the increased synthesis rate of remaining proteins and the upregulation of proteasomal proteins. *p < 0.05. All error bars represent SEM of pooled data.

upregulation of mitogenic gene networks. Thus, we directly tested our hypothesis that β cells with reduced insulin synthesis might be stimulated to enter the cell cycle and proliferate. Remarkably, insulin gene knockout β cells, marked by GFP from the mTmG reporter, proliferated at ~2 times the rate of control β cells (Figures 6A and 6B), with no measurable effect on β cell death (Figure 6C). Since increased proliferation was observed only 6 days after tamoxifen, when β cells still contained ample insulin protein, and fasting insulin and glucose were normal (Figure 1), we inferred that it was not driven by robust hyperglycemia in this model and could therefore be cell autonomous. Moreover, α cell proliferation and α cell mass were unchanged at this time point (Figures 6D and 6E), further suggesting that the induced β cell proliferation may be cell intrinsic with insulin biosynthesis being a direct negative regulator of β cell proliferation. Notably, immature embryonic β cells from *Ins1*$^{-/-}$:*Ins2*$^{-/-}$ mice also exhibited increased β cell proliferation (Duvillié et al., 2002); since embryonic glucose homeostasis is controlled by maternal insulin, this finding further supports a cell-autonomous role for insulin production in the cell cycle of developing β cells. However, the minor glucose intolerance at 6 days post-tamoxifen did not allow us to formally exclude the possibility that small changes in extracellular glucose mediated the increased proliferation we observed. Hyperglycemia and "insulin demand" have been suggested to directly mediate β cell proliferation in other models (Porat et al., 2011; Sharma et al., 2015). Thus, we devised a series of studies to directly test whether the effect of insulin gene knockout on proliferation was cell autonomous and independent of circulating glucose and insulin levels. First, we took advantage of the fact that some islets in some normoglycemic *Ins1*$^{-/-}$:*Ins2*$^{f/f}$:*Pdx1*Cre^{ERT}:mTmG mice without tamoxifen injection exhibited spontaneous partial recombination. In these mice, GFP-positive β cells were significantly more likely to be proliferating when compared to GFP-negative β cells within the same islets, experiencing identical extracellular glucose and insulin (Figures 6F and 6G). Notably, PCNA-positive proliferating β cells

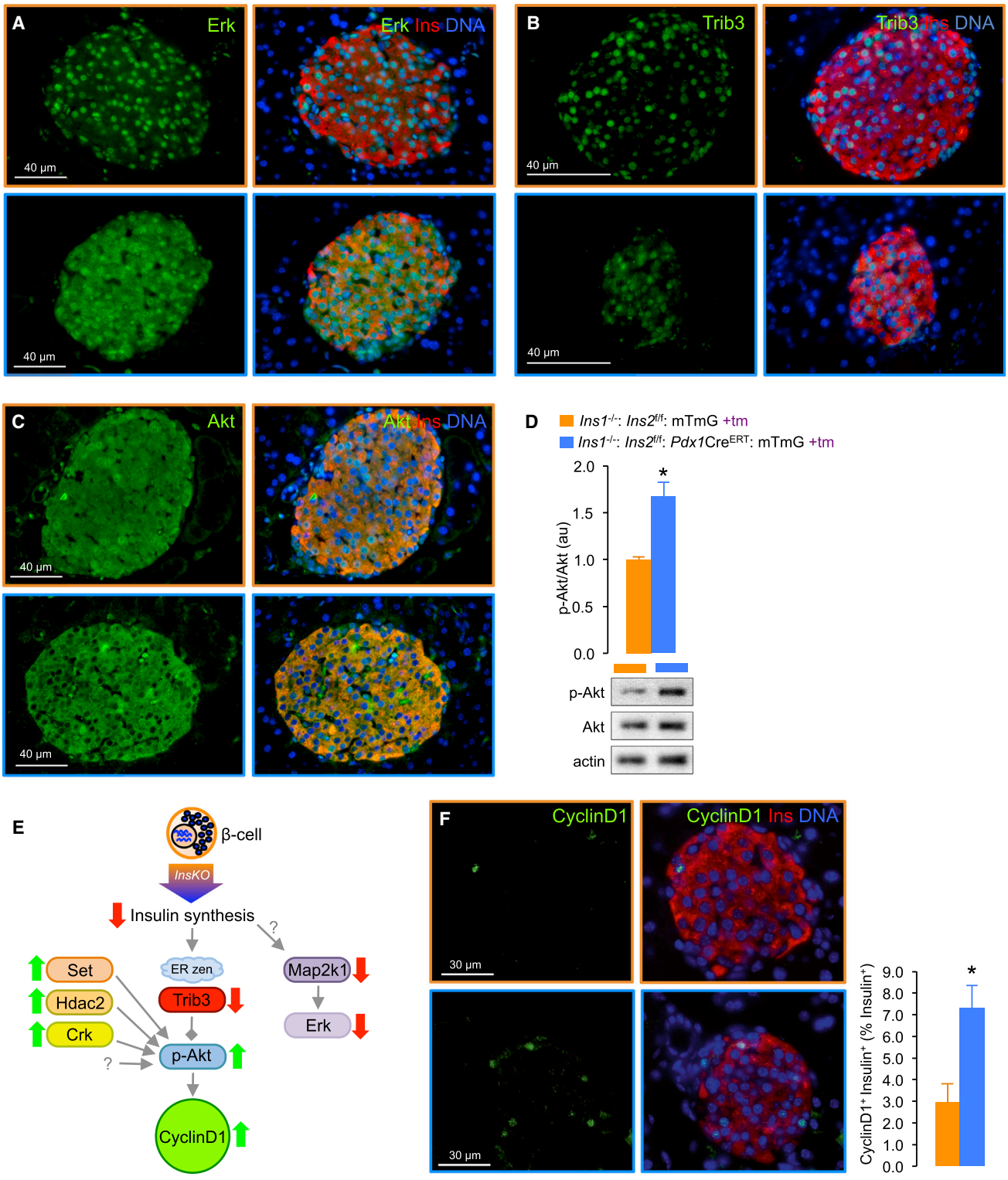

Figure 5. Akt Biased Signal Transduction in Islets with Reduced Insulin Production

(A) Altered in vivo localization of Erk1/2 in pancreas section (representative image, n = 3).

(B) Trib3 immunoreactivity in pancreas section (representative image, n = 3).

(C) In vivo localization of Akt in pancreas section (representative image, n = 3).

(D) Quantification of serine 473 phosphorylation of Akt by immunoblot in isolated islets (n = 16).

(legend continued on next page)

exhibited significantly reduced insulin staining intensity on average in these partially recombined islets (Figure 6H). Second, we co-transplanted 50 *Ins1*$^{-/-}$:*Ins2*$^{f/f}$:*Pdx1*Cre^{ERT}:mTmG islets and 50 *Ins1*$^{-/-}$:*Ins2*$^{f/f}$:mTmG control islets into the same anterior eye chamber of recipient mice that were then injected with tamoxifen and remained normoglycemic for the duration of the experiment (fasted blood glucose before graft harvest was 6.3 ± 0.4 mM). Again, we observed significantly increased β cell proliferation in insulin gene knockout β cells (marked by GFP), when compared to adjacent co-transplanted GFP-negative *Ins1*$^{-/-}$:*Ins2*$^{f/f}$:mTmG control cells within the same eye graft (Figures 6I and 6J). Third, we compared cells within the same in vitro cultures of dispersed islets with partial recombination and observed a significant increase in the proliferation rate (this time measured with EdU incorporation) of GFP-positive insulin gene knockout β cells, relative to GFP-negative control β cells (Figures 6K and 6L). Collectively, these experiments strongly suggest that reduced insulin production drives β cell proliferation in a cell-autonomous manner, independently of changes in extracellular glucose or insulin. In vitro studies of human β cell lines clearly illustrate the converse cell-autonomous effect (i.e., that inhibition of proliferation in sub-differentiated cells dramatically increases insulin production) (Scharfmann et al., 2014). We propose that multiple parallel pathways contribute to drive proliferation in β cells with reduced insulin production. Usually, proliferation is kept at very low levels in fully functional mature β cells (Beith et al., 2008; Mezza and Kulkarni, 2014; Teta et al., 2005), and it appears from our results that sub-threshold chronic ER stress associated with the normal high rate of insulin production is among the many factors that can act as a brake on proliferation. In our study, relief from ER stress was associated with reduced *Ddit3*, and knockout of this critical transcription factor is sufficient to increase β cell proliferation in *db/db* mice (Song et al., 2008). Higher ATP levels in insulin gene knockout islets likely facilitate increased proliferation. Recently, Alonso and colleagues reported that mild ER stress is associated with increased β cell proliferation in the context of sustained hyperglycemia, and that this effect could be reversed by ATF6 and IRE1 inhibitors, but not an inhibitor of the PERK pathway (Sharma et al., 2015). It appears that ER stress has complex context-dependent and pathway-specific links to the β cell proliferative machinery.

Cell Identity Confusion and Eventual De-Differentiation in Insulin Gene Knockout Islets

Finally, we assessed whether the loss of insulin production might affect β cell identity, directly or indirectly (Szabat et al., 2012) (Figures 7A–7C). Examination 6 days after tamoxifen initiation revealed that 3.8% ± 0.4% of glucagon-positive cells co-expressed GFP but not insulin, but this was not significantly higher than the background rate of recombination in islets without insulin gene knockout, suggesting it was not caused by a cell-autonomous loss of insulin production (Figures 7A and 7C). However, after 34 days, including ~2 weeks of diabetes caused by dramatic loss of pancreatic insulin stores (Figures 7B and 7D), 8.3% ± 0.5% of glucagon-positive cells expressed GFP (Figure 7C). Many of the glucagon-positive cells were found in the islet core (Figure 7B), suggesting they may have converted from β cells that normally reside in the center of mouse islets. After 34 days, glucagon-positive area in histological pancreatic sections was more than doubled (Figure 7E), as was islet glucagon mRNA (Figure 7F). At the 34 day time point, we observed significant "islet de-differentiation" with reduced *Pdx1*, *MafA*, and other markers of mature β cells (Figure 7F). At this late hyperglycemic stage, the altered islet architecture and increased glucagon expression appears remarkably similar to islets after β-cell-specific *Pdx1* knockout, including the dramatic loss of the same mature β cell markers (Gao et al., 2014). Given that hyperglycemia has previously been implicated in glucagon mis-expression (Brereton et al., 2014; Gao et al., 2014; Talchai et al., 2012), it seems a likely culprit for contributing to the apparent mis-expression of glucagon in a sub-population of insulin gene knockout β cells. While the exact mechanisms of this phenomenon remain to be identified, it is notable that β cell phenotypic plasticity has been previously observed in β cells lacking adaptive PERK-mediated phosphorylation of eIF2α (Kaufman et al., 2010), as well as cells overexpressing constitutively active Akt (Elghazi et al., 2009).

In summary, we present the first direct evidence that normally high insulin production directly suppresses β cell proliferation associated with sub-threshold chronic ER stress and is required to maintain β cell identity indirectly via glucose homeostasis. Mechanistically, we define protein networks associated with the loss of insulin production and identify new candidate factors that may accelerate efforts to induce β cell proliferation. These fundamental studies shed light on the molecular sequelae of reduced insulin production associated with diabetes (Yang et al., 2011a).

EXPERIMENTAL PROCEDURES

Animals and In Vivo Physiology

Animal protocols were performed in accordance with the University of British Columbia Animal Care Committee. *Ins1*$^{-/-}$:*Ins2*^{fff} mice have been described (Fan et al., 2009). *Pdx1*CreERT mice (Gu et al., 2002) were purchased from Jax (stock # 024968). Mice carrying the lineage tracing marker membrane-targeted tomato/membrane-targeted GFP (Muzumdar et al., 2007) were purchased from Jax (stock # 007675). Mice (6–8 weeks old) were injected intraperioneally with tamoxifen (3 mg/40 g body weight), dissolved in corn oil, for 4 consecutive days. Basal blood glucose and insulin were measured after a 4 hr fast. Glucose tolerance, insulin secretion, or insulin tolerance were assessed in mice injected with either 200 mg/ml (20%) glucose or 1.5 U/kg body weight insulin after a 4 hr fast. Insulin from in vivo samples was measured using ELISA kits from Alpco.

Islet Transplantation and Tissue Processing

To examine possible effects of blood glucose on the increased proliferation and glucagon mis-expression in insulin knockout β cells, islets from control

(E) Working model of shifted signaling in islets with reduced insulin production, illustrating the multiple positive influences on Akt activation and CyclinD1 activation.

(F) CyclinD1 immunoreactivity in β cells. (Representative image, n = 3.) *p < 0.05. Orange and blue borders around immunofluorescence images represent *Ins1*$^{-/-}$:*Ins2*$^{f/f}$:mTmG controls and *Ins1*$^{-/-}$:*Ins2*$^{f/f}$:*Pdx1*Cre^{ERT}:mTmG experimental samples, respectively. All error bars represent SEM of pooled data.

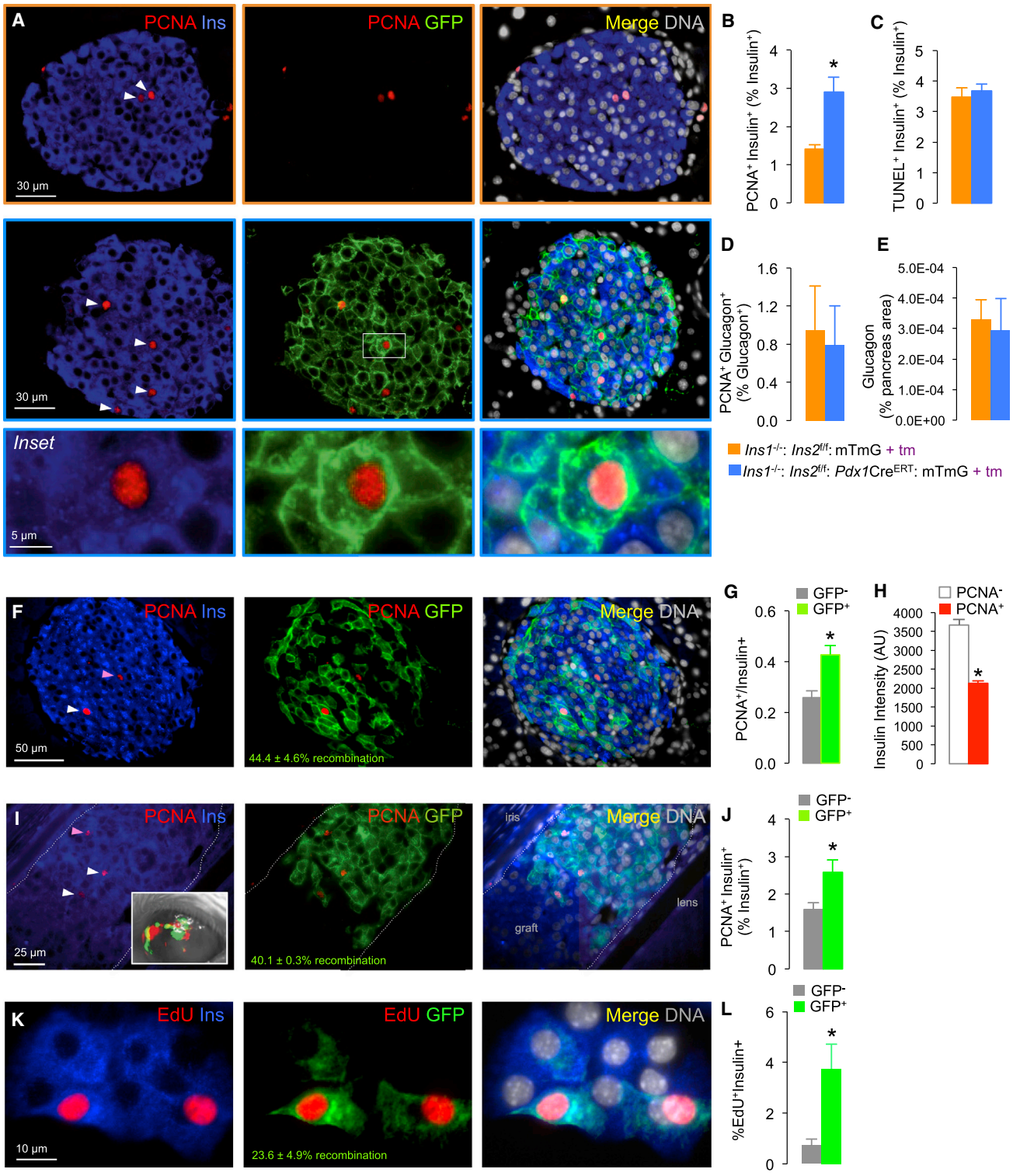

Figure 6. Cell-Autonomous Increase in β Cell Proliferation after Reduced Insulin Production

(A and B) PCNA, insulin, and GFP immunofluorescent staining in β cells in littermate controls *Ins1*$^{-/-}$:*Ins2*$^{f/f}$:mTmG (no tamoxifen) and *Ins1*$^{-/-}$:*Ins2*$^{f/f}$::*Pdx1*Cre^{ERT}: mTmG (insulin gene knockout) pancreata, 6 days following the initial tamoxifen dose, and quantification of β cell proliferation (n = 3).

(C) Number of TUNEL-positive β cells (n = 3).

(D) Quantification of α cell proliferation from the same mice (n = 3).

(E) Pancreatic glucagon-positive area at the 6-day time point (n = 3).

(legend continued on next page)

and experimental animals were co-transplanted into normoglycemic recipient mice to maintain the same exposure to glucose and insulin. A mixture of equal numbers of 50 hand-picked islets isolated from donor control mice (*Ins1*$^{-/-}$: *Ins2*^{flf}: mTmG) and donor insulin knockout mice (*Ins1*$^{-/-}$:*Ins2*^{flf}: *Pdx1*CreERT: mTmG) were co-transplanted into age-matched recipient NOD-SCID mice into the anterior chamber of the eye (Mojibian et al., 2013).

Ten days after transplantation, animals were injected intraperioneally with tamoxifen (3 mg/40 g body weight), dissolved in corn oil, for 4 consecutive days. Graft tissues were harvested 3 weeks post-tamoxifen initiation. Eyes with engrafted islets were placed in Davidson's fixative (two parts 37% formalin, three parts 100% ethanol, one part glacial acetic acid, and three parts tap water) for 24 hr at 4°C, then transferred to 70% ethanol for storage. Tissues were processed into 5 μm paraffin sections and mounted by Wax-it Histology Services (Vancouver, Canada).

Immunohistochemistry

Pancreata from PBS perfused mice were harvested and fixed in 4% paraformaldehyde for 24 hr before being washed and stored in 70% ethanol, prior to paraffin embedding. Pancreatic sections (5 μm) were taken from at least three different regions of the pancreas 100 μm apart. Sections were deparaffinized, hydrated with decreasing concentrations of ethanol, and rinsed with PBS. Sections were subjected to 15 min of heat-induced epitope retrieval at 95°C using a 10 mM citrate buffer, pH 6.0. Sections were blocked then incubated with primary antibodies overnight in a humid chamber at 4°C. A list of primary antibodies can be found in Table S5. Primary antibodies were visualized following incubation with secondary antibodies conjugated to AlexaFluor 488, 555, 594, or 647 as required (1:1,000; Invitrogen) or using anti-guinea pig AMCA (1:250; Jackson Immunologicals). TUNEL reactivity was detected using the In Situ Cell Death Kit (Roche). Images for β cell and α cell area were taken on ImageXpress^{MICRO} using a 10× (NA 0.3) objective and analyzed using the MetaXpress software (Molecular Devices Corporation). All other images were taken on a Zeiss 200M microscope using 20× air (NA 0.75), 40× oil (NA 1.3), and/or 100× oil (NA 1.45) objectives and analyzed using Slidebook software.

Electron Microscopy

Pancreas tissue from control and experimental mice at 6 days post-tamoxifen initiation were cut into small pieces and stored in 2% glutaraldehyde diluted in PBS. Samples were processed by the Electron Microscopy Facility at McMaster University, Faculty of Health Sciences (Hamilton). The samples were rinsed twice in 0.1 M phosphate buffer pH 7.4 and post-fixed in 1% osmium tetroxide in 0.1 M phosphate buffer for 1 hr. The samples were dehydrated through a graded ethanol series with final dehydration in propylene oxide, then infiltrated and embedded with Spurr's resin. Thin sections were cut on a Leica UCT Ultramicrotome, picked up onto Cu grids, then post-stained with uranyl acetate and lead citrate and viewed in a JEOL JEM 1200 EX TEMSCAN transmission electron microscope (JEOL) operating at an accelerating voltage of 80 kV. The images were acquired with an AMT 4 megapixel digital camera (Advanced Microscopy Techniques).

Islet Isolation and Culture

Pancreatic islets were isolated using collagenase, filtration, and hand-picking as described (Szabat et al., 2010). Islets were cultured overnight (37°C, 5% CO_2) in RPMI1640 medium (Invitrogen) with 11 mM glucose (Sigma), 100 units/ml penicillin, 100 μg/ml streptomycin (Invitrogen), and 10% vol/vol FBS (Invitrogen). Real-time RT-PCR and western blotting were conducted as described previously (Szabat et al., 2010; Yang et al., 2011b). Lists of antibodies and primers used can be found in Tables S5 and S6.

Multi-Omics Analysis

Detailed methods for the RNA sequencing, mass spectroscopy-based proteomics, and metabolomics are provided in the Supplemental Experimental Procedures. Briefly, RNA sequencing was conducted with HiSeq2500, collecting >20 million nucleotide 150 bp paired-end reads. TopHat2 was used to align reads to the GRCm38_68 reference genome. Expression levels were quantified with RNA-SeQC in *strictMode* and differential expression analysis was performed on the gene-level read count data using the limma empirical Bayes analysis pipeline with voom precision weights for normalization. After correcting for multiple testing, a q value < 0.001 was deemed significant. Raw and processed RNA sequencing data have been submitted to GEO (GEO: GSE74113). Briefly, proteomic analysis employed LC/MS/MS and obtained a partial proteome of ~3,000 high-confidence proteins (identified via at least two independent peptide spectra). The study was repeated three times with separate biological replicates. We excluded any proteins for which we only had readings in one biological replicate. We excluded proteins for which there was poor agreement between biological replicate runs (SD > 50% of the average intensity measurement). Results were plotted as log2 fold change. Results were analyzed using Genemania, Panther, Reactome, and DAVID. Network analysis was conducted as described in the Supplemental Experimental Procedures. Metabolomics analyses were conducted by ultra-performance liquid chromatography-tandem mass spectrometry.

Statistical Analysis

Unless otherwise indicated, data are expressed as mean ± SEM. Results were considered statistically significant when $p < 0.05$ using two-tailed, unpaired Student t test, unless otherwise indicated.

SUPPLEMENTAL INFORMATION

Supplemental Information includes six tables and Supplemental Experimental Procedures and can be found with this article online at http://dx.doi.org/10.1016/j.cmet.2015.10.016.

AUTHOR CONTRIBUTIONS

M.S. designed experiments, performed experiments, analyzed data, and co-wrote the manuscript. M.M.P., E.P., S. Skovsø, M.M., J.F.-T., and J.H. designed experiments, performed experiments, analyzed data, and edited the manuscript. J.E.B. analyzed data, and edited the manuscript. M.J.B., J.T.C.L., E.E.X., K.-M.M., and S. Sinha performed experiments, analyzed data, and edited the manuscript. F.T. and S.O.'D. performed experiments. M.v.d.B. analyzed data and edited the manuscript. Y.F. and M.T. provided essential research tools and edited the manuscript. F.C.L. designed studies, analyzed data, and edited the manuscript. C.H.B., L.J.F., C.N., and T.J.K. designed experiments; oversaw experiments; and edited the manuscript. J.D.J. conceptualized and designed studies, performed analysis, co-wrote the manuscript, and takes full responsibility for its contents.

(F and G) Cell-by-cell analysis of β cell proliferation within the same islets with partial spontaneous recombination (n = 3 pancreata; >2,000 GFP-positive and GFP-negative cells counted per n from islets with ~40%–50% recombination).
(H) Proliferating (PCNA-positive) β cells exhibited lower insulin staining intensity than non-proliferating β cells (n = 3).
(I and J) Increased proliferation in *Ins1*$^{-/-}$:*Ins2*$^{f/f}$:*Pdx1*Cre^{ERT}:mTmG (insulin gene knockout) β cells (green) compared with β cells from *Ins1*$^{-/-}$:*Ins2*$^{f/f}$:mTmG control islets co-transplanted side-by-side into normoglycemic recipient mice injected with tamoxifen (n = 4 recipients, 8 paired control and experimental islet donors—2 donors per recipient; >2,000 GFP-positive and GFP-negative cells counted per replicate).
(K and L) Increased proliferation (EdU incorporation) in insulin gene knockout β cells (green) from dispersed islets with spontaneous partial recombination compared with control non-recombined β cells cultured in the same dish in 5 mM glucose containing media (n = 3 independent islet isolations; similar islets as [F] and [G]). *$p < 0.05$. White arrowheads: PCNA-positive β cells (marked by insulin-positive and/or GFP-positive staining); pink arrowheads: PCNA-positive/insulin-positive/GFP-negative β cells. Orange and blue borders around immunofluorescence images represent *Ins1*$^{-/-}$:*Ins2*$^{f/f}$:mTmG controls and *Ins1*$^{-/-}$:*Ins2*$^{f/f}$:*Pdx1*Cre^{ERT}:mTmG experimental samples, respectively. All error bars represent SEM of pooled data.

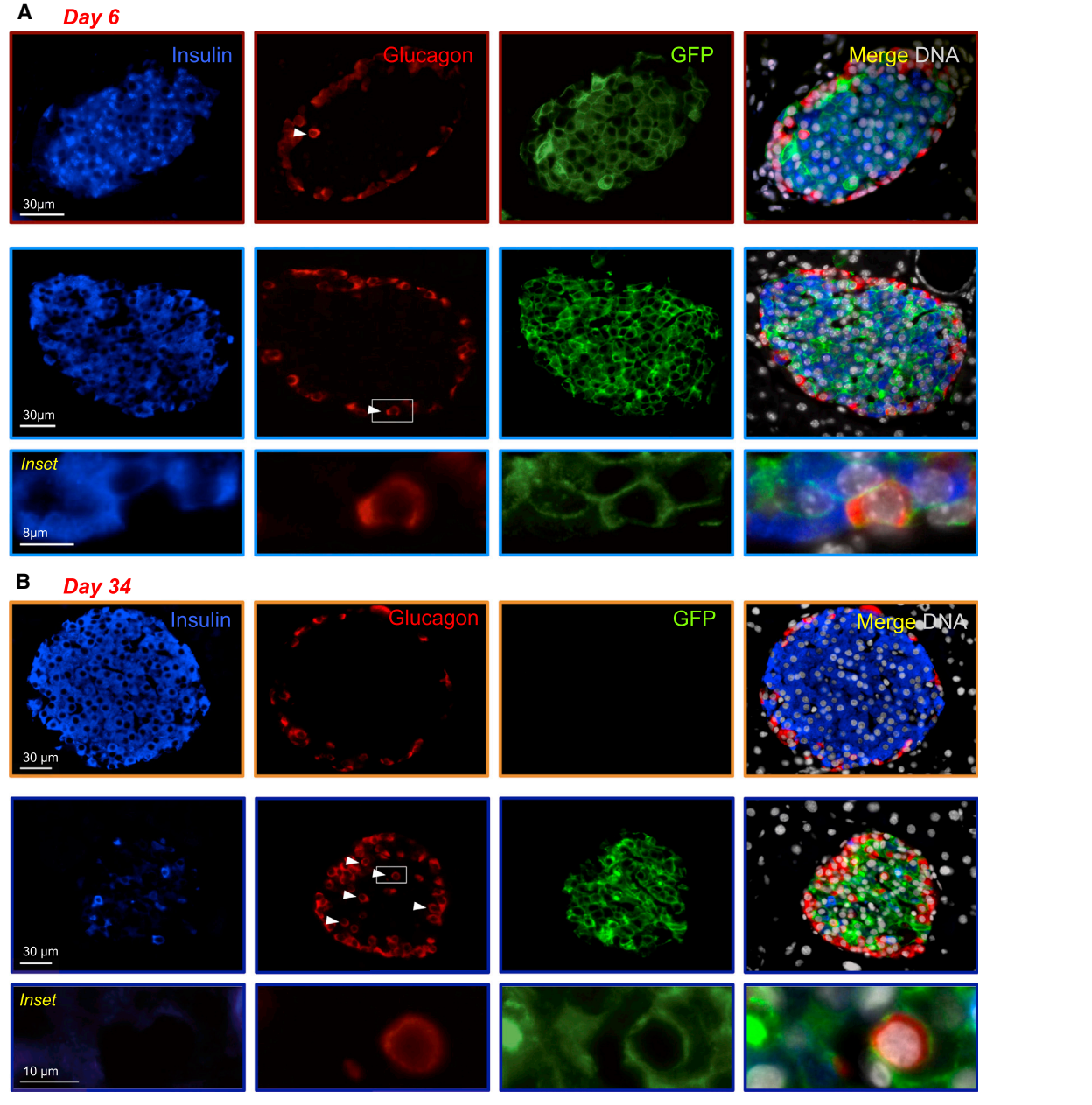

(legend on next page)

CONFLICTS OF INTEREST

None of the authors have any conflicts of interest to disclose.

ACKNOWLEDGMENTS

We thank Dr. Alireza Rezania (BetaLogics) for the generous gift of MafA antibody. We thank Micah Piske and Betty Hu for their expert technical help and Dr. Tobias Boothe for assistance with RNAseq analysis and a careful reading of the manuscript. We thank Marcia Reid of the McMaster University Electron Microscopy Facility for expert imaging work. We thank Dr. Eric Jan for assistance with S35 labeling, and for reading the manuscript. We thank Dr. Elizabeth Rideout for reading of the manuscript. We appreciate the constructive comments from the peer reviewers and many colleagues that improved the study.

This study was funded by grants from the JDRF and the Canadian Diabetes Association (CDA). M.S., J.E.B., and M.M.P. were supported by CDA Postdoctoral Fellowships. M.S. and E.P. were supported by CIHR Transplant Training Post-doctoral Fellowships. This research was enabled in part by support provided by WestGrid (https://www.westgrid.ca) and Compute Canada/Calcul Canada (https://www.computecanada.ca).

Received: April 15, 2015
Revised: September 13, 2015
Accepted: October 25, 2015
Published: November 25, 2015

REFERENCES

Akagi, T., Shishido, T., Murata, K., and Hanafusa, H. (2000). v-Crk activates the phosphoinositide 3-kinase/AKT pathway in transformation. Proc. Natl. Acad. Sci. USA *97*, 7290–7295.

Akirav, E., Kushner, J.A., and Herold, K.C. (2008). Beta-cell mass and type 1 diabetes: going, going, gone? Diabetes *57*, 2883–2888.

Back, S.H., and Kaufman, R.J. (2012). Endoplasmic reticulum stress and type 2 diabetes. Annu. Rev. Biochem. *81*, 767–793.

Beith, J.L., Alejandro, E.U., and Johnson, J.D. (2008). Insulin stimulates primary beta-cell proliferation via Raf-1 kinase. Endocrinology *149*, 2251–2260.

Bernal-Mizrachi, E., Wen, W., Stahlhut, S., Welling, C.M., and Permutt, M.A. (2001). Islet beta cell expression of constitutively active Akt1/PKB alpha induces striking hypertrophy, hyperplasia, and hyperinsulinemia. J. Clin. Invest. *108*, 1631–1638.

Brereton, M.F., Iberl, M., Shimomura, K., Zhang, Q., Adriaenssens, A.E., Proks, P., Spiliotis, I.I., Dace, W., Mattis, K.K., Ramracheya, R., et al. (2014). Reversible changes in pancreatic islet structure and function produced by elevated blood glucose. Nat. Commun. *5*, 4639.

Chera, S., Baronnier, D., Ghila, L., Cigliola, V., Jensen, J.N., Gu, G., Furuyama, K., Thorel, F., Gribble, F.M., Reimann, F., and Herrera, P.L. (2014). Diabetes recovery by age-dependent conversion of pancreatic δ-cells into insulin producers. Nature *514*, 503–507.

Chu, K.Y., Li, H., Wada, K., and Johnson, J.D. (2012). Ubiquitin C-terminal hydrolase L1 is required for pancreatic beta cell survival and function in lipotoxic conditions. Diabetologia *55*, 128–140.

Cromer, M.K., Choi, M., Nelson-Williams, C., Fonseca, A.L., Kunstman, J.W., Korah, R.M., Overton, J.D., Mane, S., Kenney, B., Malchoff, C.D., et al. (2015). Neomorphic effects of recurrent somatic mutations in Yin Yang 1 in insulin-producing adenomas. Proc. Natl. Acad. Sci. USA *112*, 4062–4067.

Dror, V., Nguyen, V., Walia, P., Kalynyak, T.B., Hill, J.A., and Johnson, J.D. (2007). Notch signalling suppresses apoptosis in adult human and mouse pancreatic islet cells. Diabetologia *50*, 2504–2515.

Du, K., Herzig, S., Kulkarni, R.N., and Montminy, M. (2003). TRB3: a tribbles homolog that inhibits Akt/PKB activation by insulin in liver. Science *300*, 1574–1577.

Duvillié, B., Currie, C., Chrones, T., Bucchini, D., Jami, J., Joshi, R.L., and Hill, D.J. (2002). Increased islet cell proliferation, decreased apoptosis, and greater vascularization leading to beta-cell hyperplasia in mutant mice lacking insulin. Endocrinology *143*, 1530–1537.

Elghazi, L., Weiss, A.J., Barker, D.J., Callaghan, J., Staloch, L., Sandgren, E.P., Gannon, M., Adsay, V.N., and Bernal-Mizrachi, E. (2009). Regulation of pancreas plasticity and malignant transformation by Akt signaling. Gastroenterology *136*, 1091–1103.

Enchev, R.I., Schulman, B.A., and Peter, M. (2015). Protein neddylation: beyond cullin-RING ligases. Nat. Rev. Mol. Cell Biol. *16*, 30–44.

Fan, Y., Rudert, W.A., Grupillo, M., He, J., Sisino, G., and Trucco, M. (2009). Thymus-specific deletion of insulin induces autoimmune diabetes. EMBO J. *28*, 2812–2824.

Fatrai, S., Elghazi, L., Balcazar, N., Cras-Méneur, C., Krits, I., Kiyokawa, H., and Bernal-Mizrachi, E. (2006). Akt induces beta-cell proliferation by regulating cyclin D1, cyclin D2, and p21 levels and cyclin-dependent kinase-4 activity. Diabetes *55*, 318–325.

Gao, T., McKenna, B., Li, C., Reichert, M., Nguyen, J., Singh, T., Yang, C., Pannikar, A., Doliba, N., Zhang, T., et al. (2014). Pdx1 maintains β cell identity and function by repressing an α cell program. Cell Metab. *19*, 259–271.

Gu, G., Dubauskaite, J., and Melton, D.A. (2002). Direct evidence for the pancreatic lineage: NGN3+ cells are islet progenitors and are distinct from duct progenitors. Development *129*, 2447–2457.

Guo, S., Dai, C., Guo, M., Taylor, B., Harmon, J.S., Sander, M., Robertson, R.P., Powers, A.C., and Stein, R. (2013). Inactivation of specific β cell transcription factors in type 2 diabetes. J. Clin. Invest. *123*, 3305–3316.

Halban, P.A. (1982). Differential rates of release of newly synthesized and of stored insulin from pancreatic islets. Endocrinology *110*, 1183–1188.

Ivanova, A., Kalaidzidis, Y., Dirkx, R., Sarov, M., Gerlach, M., Schroth-Diez, B., Müller, A., Liu, Y., Andree, C., Mulligan, B., et al. (2013). Age-dependent labeling and imaging of insulin secretory granules. Diabetes *62*, 3687–3696.

Kaufman, R.J., Back, S.H., Song, B., Han, J., and Hassler, J. (2010). The unfolded protein response is required to maintain the integrity of the endoplasmic reticulum, prevent oxidative stress and preserve differentiation in β-cells. Diabetes Obes. Metab. *12* (*Suppl 2*), 99–107.

Kushner, J.A., Ciemerych, M.A., Sicinska, E., Wartschow, L.M., Teta, M., Long, S.Y., Sicinski, P., and White, M.F. (2005). Cyclins D2 and D1 are essential for postnatal pancreatic beta-cell growth. Mol. Cell. Biol. *25*, 3752–3762.

Lim, G.E., Piske, M., and Johnson, J.D. (2013). 14-3-3 proteins are essential signalling hubs for beta cell survival. Diabetologia *56*, 825–837.

Figure 7. Glucagon Production in Recombined Cells and Islet Dedifferentiation after Hyperglycemia

(A) Glucagon immunoreactivity in a subset of GFP-positive cells (inset and arrow) in control *Ins1*$^{-/-}$:*Ins2*$^{+/+}$:*Pdx1*Cre^{ERT}:mTmG islets and *Ins1*$^{-/-}$:*Ins2*$^{f/f}$:*Pdx1*Cre^{ERT}:mTmG insulin gene knockout islets at 6 days after tamoxifen initiation.

(B) Glucagon immunoreactivity in a subset of GFP-positive cells (inset and arrows) in control *Ins1*$^{-/-}$:*Ins2*$^{f/f}$:mTmG islets and *Ins1*$^{-/-}$:*Ins2*$^{f/f}$:*Pdx1*Cre^{ERT}:mTmG insulin gene knockout islets at 34 days after tamoxifen initiation.

(C) Quantification of glucagon-positive and GFP-positive cells in insulin gene knockout islets at 6 days (near normoglycemic conditions) and 34 days (hyperglycemic conditions), as well as islets from control mice with wild-type *Ins2* alleles (n = 3).

(D) Percentage insulin-positive area relative to pancreas area at 34 days.

(E) Percentage glucagon-positive area relative to pancreas area at 34 days.

(F) qPCR analysis of islet cell genes at 34 days (n = 3). *p < 0.05. Orange and blue borders around immunofluorescence images represent *Ins1*$^{-/-}$:*Ins2*$^{f/f}$:mTmG controls and *Ins1*$^{-/-}$:*Ins2*$^{f/f}$:*Pdx1*Cre^{ERT}:mTmG experimental samples, respectively. All error bars represent SEM of pooled data.

Lim, G.E., Albrecht, T., Piske, M., Sarai, K., Lee, J.T., Ramshaw, H.S., Sinha, S., Guthridge, M.A., Acker-Palmer, A., Lopez, A.F., et al. (2015). 14-3-3ζ coordinates adipogenesis of visceral fat. Nat. Commun. *6*, 7671.

Mezza, T., and Kulkarni, R.N. (2014). The regulation of pre- and post-maturational plasticity of mammalian islet cell mass. Diabetologia *57*, 1291–1303.

Mojibian, M., Harder, B., Hurlburt, A., Bruin, J.E., Asadi, A., and Kieffer, T.J. (2013). Implanted islets in the anterior chamber of the eye are prone to autoimmune attack in a mouse model of diabetes. Diabetologia *56*, 2213–2221.

Muzumdar, M.D., Tasic, B., Miyamichi, K., Li, L., and Luo, L. (2007). A global double-fluorescent Cre reporter mouse. Genesis *45*, 593–605.

Nir, T., Melton, D.A., and Dor, Y. (2007). Recovery from diabetes in mice by beta cell regeneration. J. Clin. Invest. *117*, 2553–2561.

Noh, J.H., Bae, H.J., Eun, J.W., Shen, Q., Park, S.J., Kim, H.S., Nam, B., Shin, W.C., Lee, E.K., Lee, K., et al. (2014). HDAC2 provides a critical support to malignant progression of hepatocellular carcinoma through feedback control of mTORC1 and AKT. Cancer Res. *74*, 1728–1738.

Ohoka, N., Yoshii, S., Hattori, T., Onozaki, K., and Hayashi, H. (2005). TRB3, a novel ER stress-inducible gene, is induced via ATF4-CHOP pathway and is involved in cell death. EMBO J. *24*, 1243–1255.

Pandey, D., Hori, D., Kim, J.H., Bergman, Y., Berkowitz, D.E., and Romer, L.H. (2015). NEDDylation promotes endothelial dysfunction: a role for HDAC2. J. Mol. Cell. Cardiol. *81*, 18–22.

Porat, S., Weinberg-Corem, N., Tornovsky-Babaey, S., Schyr-Ben-Haroush, R., Hija, A., Stolovich-Rain, M., Dadon, D., Granot, Z., Ben-Hur, V., White, P., et al. (2011). Control of pancreatic β cell regeneration by glucose metabolism. Cell Metab. *13*, 440–449.

Sabatini, P.V., Krentz, N.A., Zarrouki, B., Westwell-Roper, C.Y., Nian, C., Uy, R.A., Shapiro, A.M., Poitout, V., and Lynn, F.C. (2013). Npas4 is a novel activity-regulated cytoprotective factor in pancreatic β-cells. Diabetes *62*, 2808–2820.

Scharfmann, R., Pechberty, S., Hazhouz, Y., von Bülow, M., Bricout-Neveu, E., Grenier-Godard, M., Guez, F., Rachdi, L., Lohmann, M., Czernichow, P., and Ravassard, P. (2014). Development of a conditionally immortalized human pancreatic β cell line. J. Clin. Invest. *124*, 2087–2098.

Sharma, R.B., O'Donnell, A.C., Stamateris, R.E., Ha, B., McCloskey, K.M., Reynolds, P.R., Arvan, P., and Alonso, L.C. (2015). Insulin demand regulates β cell number via the unfolded protein response. J. Clin. Invest. *125*, 3831–3846.

Song, B., Scheuner, D., Ron, D., Pennathur, S., and Kaufman, R.J. (2008). Chop deletion reduces oxidative stress, improves beta cell function, and promotes cell survival in multiple mouse models of diabetes. J. Clin. Invest. *118*, 3378–3389.

Switzer, C.H., Cheng, R.Y., Vitek, T.M., Christensen, D.J., Wink, D.A., and Vitek, M.P. (2011). Targeting SET/I(2)PP2A oncoprotein functions as a multi-pathway strategy for cancer therapy. Oncogene *30*, 2504–2513.

Szabat, M., Johnson, J.D., and Piret, J.M. (2010). Reciprocal modulation of adult beta cell maturity by activin A and follistatin. Diabetologia *53*, 1680–1689.

Szabat, M., Lynn, F.C., Hoffman, B.G., Kieffer, T.J., Allan, D.W., and Johnson, J.D. (2012). Maintenance of β-cell maturity and plasticity in the adult pancreas: developmental biology concepts in adult physiology. Diabetes *61*, 1365–1371.

Talchai, C., Xuan, S., Lin, H.V., Sussel, L., and Accili, D. (2012). Pancreatic β cell dedifferentiation as a mechanism of diabetic β cell failure. Cell *150*, 1223–1234.

Teta, M., Long, S.Y., Wartschow, L.M., Rankin, M.M., and Kushner, J.A. (2005). Very slow turnover of beta-cells in aged adult mice. Diabetes *54*, 2557–2567.

Thorel, F., Népote, V., Avril, I., Kohno, K., Desgraz, R., Chera, S., and Herrera, P.L. (2010). Conversion of adult pancreatic alpha-cells to beta-cells after extreme beta-cell loss. Nature *464*, 1149–1154.

Tillmar, L., Carlsson, C., and Welsh, N. (2002). Control of insulin mRNA stability in rat pancreatic islets. Regulatory role of a 3′-untranslated region pyrimidine-rich sequence. J. Biol. Chem. *277*, 1099–1106.

Vander Mierde, D., Scheuner, D., Quintens, R., Patel, R., Song, B., Tsukamoto, K., Beullens, M., Kaufman, R.J., Bollen, M., and Schuit, F.C. (2007). Glucose activates a protein phosphatase-1-mediated signaling pathway to enhance overall translation in pancreatic beta-cells. Endocrinology *148*, 609–617.

Wang, Z., York, N.W., Nichols, C.G., and Remedi, M.S. (2014). Pancreatic β cell dedifferentiation in diabetes and redifferentiation following insulin therapy. Cell Metab. *19*, 872–882.

Weir, G.C., Aguayo-Mazzucato, C., and Bonner-Weir, S. (2013). β-cell dedifferentiation in diabetes is important, but what is it? Islets *5*, 233–237.

Wrede, C.E., Dickson, L.M., Lingohr, M.K., Briaud, I., and Rhodes, C.J. (2002). Protein kinase B/Akt prevents fatty acid-induced apoptosis in pancreatic beta-cells (INS-1). J. Biol. Chem. *277*, 49676–49684.

Wurzenberger, C., and Gerlich, D.W. (2011). Phosphatases: providing safe passage through mitotic exit. Nat. Rev. Mol. Cell Biol. *12*, 469–482.

Yang, B.T., Dayeh, T.A., Kirkpatrick, C.L., Taneera, J., Kumar, R., Groop, L., Wollheim, C.B., Nitert, M.D., and Ling, C. (2011a). Insulin promoter DNA methylation correlates negatively with insulin gene expression and positively with HbA(1c) levels in human pancreatic islets. Diabetologia *54*, 360–367.

Yang, Y.H., Szabat, M., Bragagnini, C., Kott, K., Helgason, C.D., Hoffman, B.G., and Johnson, J.D. (2011b). Paracrine signalling loops in adult human and mouse pancreatic islets: netrins modulate beta cell apoptosis signalling via dependence receptors. Diabetologia *54*, 828–842.

Yang, Y.H., Wills, Q.F., and Johnson, J.D. (2015). A live-cell, high-content imaging survey of 206 endogenous factors across five stress conditions reveals context-dependent survival effects in mouse primary beta cells. Diabetologia *58*, 1239–1249.